Modification of surface energy in nuclear multifragmentation

A. S. Botvina,[1,2] N. Buyukcizmeci,[3] M. Erdogan,[3] J. Łukasik,[1,4] I. N. Mishustin,[5,6] R. Ogul,[1,3] and W. Trautmann[1]

[1]*Gesellschaft für Schwerionenforschung mbH, D-64291 Darmstadt, Germany*

[2]*Institute for Nuclear Research, Russian Academy of Sciences, RU-117312 Moscow, Russia*

[3]*Department of Physics, University of Selçuk, TR-42079 Konya, Turkey*

[4]*H. Niewodniczański Institute of Nuclear Physics, Pl-31342 Kraków, Poland*

[5]*Frankfurt Institute for Advanced Studies, J.W. Goethe University, D-60438 Frankfurt am Main, Germany*

[6]*Kurchatov Institute, Russian Research Center, RU-123182 Moscow, Russia*

(Received 29 June 2006; published 20 October 2006)

Within the statistical multifragmentation model we study modifications of the surface and symmetry energy of primary fragments in the freeze-out volume. The ALADIN experimental data on multifragmentation obtained in reactions induced by high-energy projectiles with different neutron richness are analyzed. We have extracted the isospin dependence of the surface energy coefficient at different degrees of fragmentation. We conclude that the surface energy of hot fragments produced in multifragmentation reactions differs from the values extracted for isolated nuclei at low excitation. At high fragment multiplicity, it becomes nearly independent of the neutron content of the fragments.

DOI: 10.1103/PhysRevC.74.044609 PACS number(s): 25.70.Pq, 25.70.Mn, 21.65.+f

I. INTRODUCTION

A breakup of nuclei into many fragments (multifragmentation) has been observed in nearly all types of nuclear reactions when a large amount of energy is deposited in nuclei. This breakup includes reactions induced by protons, pions, and antiprotons and by heavy ions of both relativistic energies (peripheral collisions) and Fermi energies (central collisions). According to the present understanding, multifragmentation is a relatively fast process, with a characteristic time around 100 fm/c, where, nevertheless, a high degree of equilibration is reached. The process is mainly associated with abundant production of intermediate mass fragments (IMFs, with charges $Z \approx 3$–20). However, at the onset of multifragmentation, also heavy residues are produced that have previously only been associated with compound-nucleus processes. At very high excitation energies, the IMF production gives way to the total vaporization of nuclei into nucleons and very light clusters.

The previous ALADIN experiments have provided extensive information about multifragmentation of projectiles in peripheral nucleus-nucleus collisions at high energy [1]. They have demonstrated a rise and fall of multifragmentation with excitation energy, and they have shown that the temperature remains nearly constant, around $T \sim 5$ MeV, during this process [2]. There are large fluctuations of the fragment multiplicity and of the size of the largest fragment in the transition region from a compound-like decay to full multifragmentation of spectators [3]. It was found that the statistical models, which assume a thermal equilibration among hot fragments in a freeze-out volume at subnuclear densities, are fully consistent with the data [4–7].

We believe that multifragmentation studies pursue two main purposes. The first one is connected with the general understanding and better description of this reaction, which represents as much as 10%–15% of the total cross section in high-energy hadron-nucleus collisions, and nearly twice that in nucleus-nucleus collisions. Second, the multifragmentation reaction can be considered as an experimental tool to study the properties of hot fragments and the phase diagram of nuclear matter at densities $\rho \approx (0.1$–$0.3)\rho_0$ and temperatures around $T \approx 3$–8 MeV, which are expected to be reached in the freeze-out volume (where $\rho_0 \approx 0.15$ fm^{-3} is the normal nuclear density). Multifragmentation opens a unique possibility to investigate this part of the phase diagram and to determine the "in-medium" modifications of nuclei there. This second point is very important for many astrophysical applications, in particular, for processes during supernova type II explosions and neutron star formation [8–10].

Some of the properties of hot fragments have been addressed in our previous work. For example, the symmetry energy was extracted in Ref. [11], and it was demonstrated that it decreases considerably with excitation energy. In this paper we show that the surface energy of hot fragments can also be investigated in these reactions and that the modified surface energy can be extracted by comparing theory with experiment.

II. STATISTICAL APPROACH FOR THE DESCRIPTION OF MULTIFRAGMENTATION

Statistical models are used in situations when an equilibrated source can be defined in the nuclear reaction. The most famous example of such a source is the "compound nucleus" introduced by Niels Bohr in 1936. The standard compound nucleus picture is valid only at low excitation energies when sequential evaporation of light particles and fission are the dominating decay channels. However, this concept cannot be directly applied at high excitation energies, $E^* \gtrsim$ 2–3 MeV/nucleon, when the nucleus rapidly disintegrates into many fragments. As was shown in many experiments (see, e.g., Refs. [12–17]), an equilibrated source can be formed in this case too, and statistical models are generally very successful in describing the fragment production.

As a basis for our study we take the statistical multifragmentation model (SMM); for a review see Ref. [5]. This model considers a late freeze-out stage of the reaction where the system is still in statistical equilibrium. It is assumed that prefragments are formed in the freeze-out volume, whereas their properties may change compared to the vacuum owing to the proximity of other fragments. The residual nuclear interaction is taken into account via the excluded volume correction and modification of the liquid-drop model parameters. The statistical ensemble includes all breakup channels composed of nucleons and excited fragments and takes into account the conservation of baryon number, electric charge, and total energy. Light clusters with mass number $A \leqslant 4$ are treated as elementary particles with only translational degrees of freedom "nuclear gas"). Fragments with $A > 4$ are treated as heated liquid drops. In this way one may study the nuclear liquid-gas coexistence in the freeze-out volume. The Coulomb interaction of fragments is described within the Wigner-Seitz approximation. Different decay channels f are generated by Monte Carlo sampling according to their statistical weights, $\propto \exp S_f$, where S_f is the entropy of channel f. After the breakup, the Coulomb acceleration and the secondary de-excitation of primary hot fragments are taken into account. The SMM has been already successfully applied for the analysis of ALADIN data [12,18].

III. INFLUENCE OF THE SYMMETRY ENERGY ON MULTIFRAGMENTATION

In the SMM, the symmetry energy of hot fragments with mass number A and charge Z is parametrized as $E^{\rm sym}_{A,Z} = \gamma(A-2Z)^2/A$, where γ is a phenomenological parameter. In the case of cold nuclei $\gamma \approx 25$ MeV is adopted to describe their binding energies. For hot fragments this parameter can be modified and, therefore, should be extracted from experimental data. The corresponding set of isospin-related data may be provided by the multifragmentation reactions (e.g., via the isoscaling phenomenon [19]). At present, there is evidence for a significant reduction of the symmetry energy of hot fragments in multifragmentation [11,20].

The influence of the symmetry energy on the characteristics of produced fragments was already partly analyzed in [21]. It was shown that it has a small effect on average quantities such as the temperature and fragment masses, but it influences mainly the isotope distributions of the fragments. This is illustrated in Fig. 1 for the mean charge distributions and neutron-to-proton (N/Z) ratios of fragments. These characteristics change only slightly even with rather large variations of γ. In this respect, we believe that variations of γ will not influence the results of previous analyses of experimental data related to the fragment charge partitions and average isotope yields [5,12–18].

By contrast, the symmetry energy has a large effect on isotope distributions. As evident from Fig. 2, they become wider at small γ [19,22]. The subsequent de-excitation of the produced hot fragments changes the distributions in two ways: Their widths usually become narrower and their centroids are shifted toward symmetry [19,21,23]. This effect has to be taken into account when making comparisons with experimental data; it is essential, for example, for the isoscaling analysis [11,19,20].

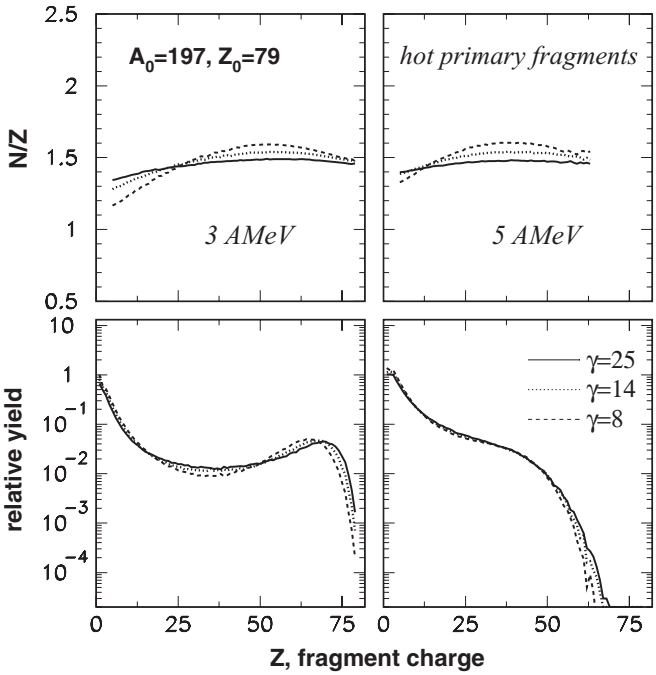

FIG. 1. Influence of the symmetry energy coefficient γ on yields of hot fragments in the freeze-out volume (bottom panels) and on their N/Z ratios (top panels) in SMM calculations for Au sources at excitation energies of 3 and 5 MeV/nucleon (left and right panels, respectively).

In the following, we study possible modifications of the fragment surface energy by employing different isospin

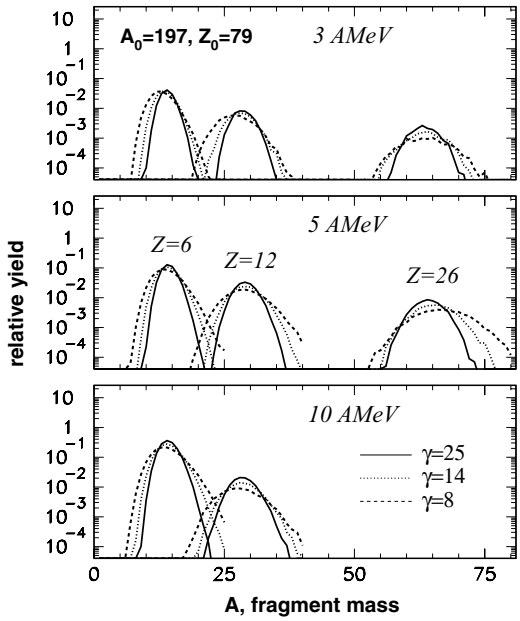

FIG. 2. Mass distributions of hot fragments with atomic numbers $Z = 6$, 12, and 26, produced in the multifragmentation of Au sources at excitation energies of 3, 5, and 10 MeV/nucleon, for different symmetry energy coefficients γ.

compositions of the sources. Within the SMM this issue can be separated from modifications of the symmetry energy because the latter does not significantly change the mean charge yields. In phenomenological mass formulas, isospin-dependent terms for the surface energy are sometimes introduced to obtain a better description of the ground-state masses of nuclei [24,25]. However, some modern mass formulas can provide even better descriptions of the nuclear masses, retaining only the bulk isospin term but with a special treatment of the shell effects [26]. We believe that the best strategy for the present purpose of investigating new "in-medium" properties of nuclear fragments is to consider a minimum number of parameters that have a clear physical meaning. We, therefore, use the standard SMM liquid-drop parametrization that contains no surface isospin term. Instead, we allow for the surface coefficient to be a free parameter that is determined by comparing the calculations with experimental data obtained for multifragmentation of nuclei with different isospin content.

IV. INFLUENCE OF THE SURFACE ENERGY ON MULTIFRAGMENTATION

The surface free energy of hot fragments in the SMM is parametrized as $F^{\rm surf}_{A,Z} = B(T)A^{2/3}$, where $B(T) = B_0[(T_c^2 - T^2)/(T_c^2 + T^2)]^{5/4}$. Here $B_0 \approx 18$ MeV is the surface coefficient for isolated cold nuclei, as adopted in the Weizsaecker mass formula, and $T_c \approx 18$ MeV is the critical temperature for the nuclear liquid-gas phase transition in infinite matter. One should distinguish T_c from the phase transition temperature in finite hot nuclei, which is essentially lower, around 5–6 MeV [5]. T_c should be considered as a model parameter characterizing the temperature dependence of the surface tension in finite nuclei. At low temperatures this T dependence leads to a correct surface contribution to the level densities of nuclei; that is, it describes correctly the heat capacities of isolated nuclei. The surface parameters may also be modified in the low-density nuclear medium (i.e., in environments consisting of nucleons and hot fragments). The possible changes of T_c in multifragmentation reactions were analyzed in Refs. [21,27,28], and from the analysis of experimental data it was found that $T_c \approx 17$–20 MeV in reactions with Au nuclei. The T_c effect on fragment yields is rather small and, in any case, it is included in the surface energy. In the present work we concentrate on the influence of the B_0 coefficient on the multifragmentation pattern.

The surface energy is rather important, since production of new fragments means increasing the surface contribution to the total energy of the system. Therefore, even small variations of the surface energy lead to big changes of fragment mass and charge distributions. This is demonstrated in Fig. 3 for different excitation energies of Au sources with a freeze-out density $\rho = \rho_0/3$. Decreasing the surface energy favors the disintegration already at low excitation energies whereas a larger B_0 suppresses the multifragmentation channels.

To characterize the charge distributions we use the $Z^{-\tau}$ fit of the fragment yields. To avoid contributions of other processes leading, for example, to fission-like large fragments ($Z > 20$) and to coalescence-like small clusters ($Z \lesssim 2$), we

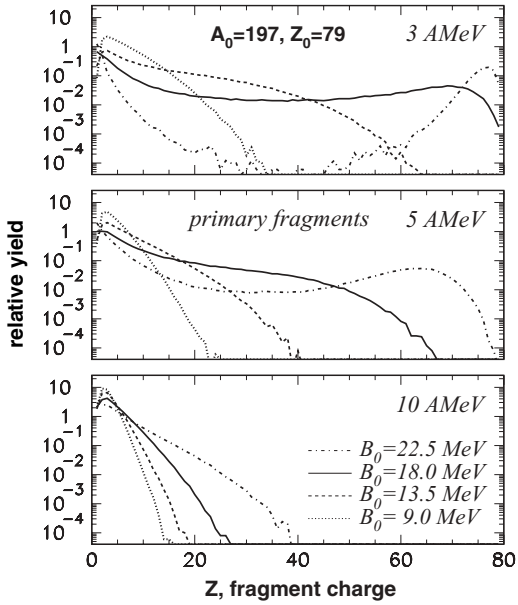

FIG. 3. Influence of the surface energy coefficient B_0 on charge yields of hot fragments in the freeze-out volume, as obtained from SMM calculations for Au sources at excitation energies of 3, 5, and 10 MeV/nucleon.

limit the fragment charges by the range $Z = 5$–15 in this fit. The extracted τ parameters for three sources with different isospin, ^{238}U, ^{197}Au, and ^{129}Xe, are shown in Fig. 4. In these calculations, the surface coefficient was fixed at the standard value of $B_0 = 18$ MeV. One can see that the isospin effect is rather essential, as was already discussed in [21,27].

We choose the Au source to demonstrate possible effects of the modified surface energy on multifragmentation. Figure 5 shows the influence of the coefficient B_0 on the caloric curve, on the mass number $A_{\rm max}$ of the largest fragment, and on τ. We should point out that thermodynamical characteristics of the system in the freeze-out volume can also be influenced by the

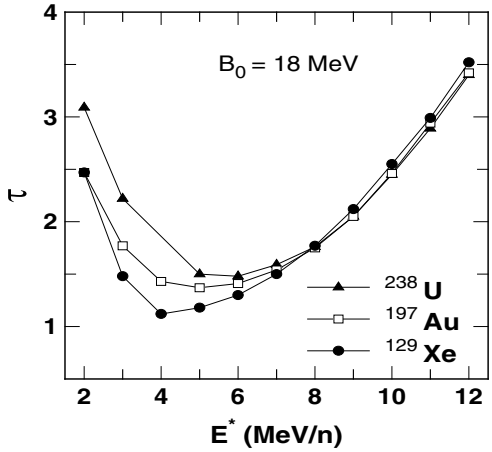

FIG. 4. SMM calculations of τ parameters for hot fragments from ^{238}U, ^{197}Au, and ^{129}Xe sources as a function of their excitation energies. The power-law fitting was performed for fragments with $Z = 5$–15.

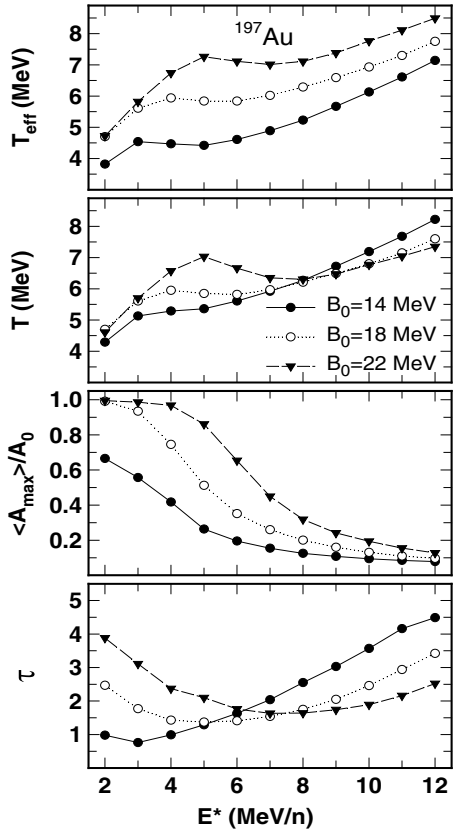

FIG. 5. SMM calculations of characteristics of hot fragments from Au sources for different surface energy coefficients $B_0 = 14, 18, 22$ MeV as a function of the excitation energy E^*. Top two panels: effective temperature $T_{\rm eff}$ and freeze-out temperature (caloric curves); middle panel: reduced mass number of the maximum fragment, $A_{\rm max}/A_0$; bottom panel: τ parameter.

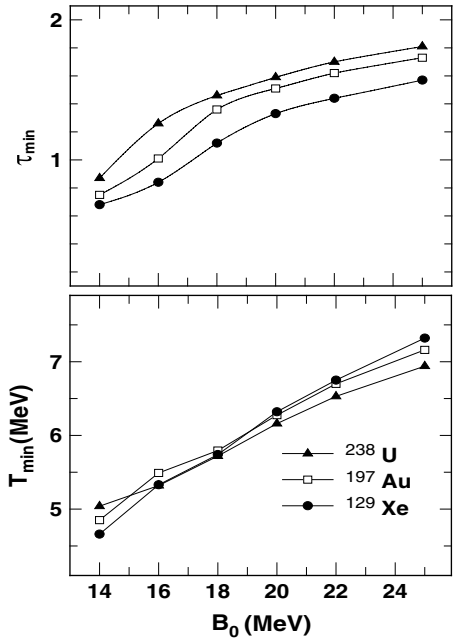

FIG. 6. Minimum value $\tau_{\rm min}$ of the τ parameter for hot fragments and the corresponding effective temperature $T_{\rm min}$, extracted from SMM calculations for sources with different neutron richness ^{238}U, ^{197}Au, and ^{129}Xe, as a function of the surface energy coefficient B_0.

modifications of the surface energy of fragments. When these hot fragments leave the freeze-out volume and decay, their normal properties are restored. To emphasize the difference between isolated nuclei and nuclei in the medium, we introduce two different temperatures. One is an effective temperature $T_{\rm eff}$, which is found from the energy balance in the freeze-out volume by assuming that the properties of fragments are the same as those of isolated nuclei. This effective temperature reflects internal excitations of fragments respective to their ground states and, thus, it can be compared to the temperature reached in the compound nucleus at the same excitation. Another temperature is the freeze-out temperature T, which includes in-medium modifications of the fragment properties (i.e., different B_0). The evolution of both temperatures with E^* is presented in Fig. 5 in the top two panels. One can see that variations in B_0 lead to noticeable effects. With a small B_0, correlated with a smaller effective temperature, the system disintegrates into lighter fragments, and $A_{\rm max}$ becomes smaller too. At low excitations the effective and freeze-out temperatures exhibit a similar behavior. However, at very high excitation energies when the system disintegrates only into light IMFs, the freeze-out temperature becomes higher at smaller B_0. This behavior has a simple explanation: The smaller surface term leads to a smaller level density parameter for internal excitation of fragments, which requires higher freeze-out temperatures to achieve the energy balance. The τ parameter exhibits a general trend in the evolution of the charge distributions, depending strongly on the excitation energy for all considered values of the surface coefficient (Fig. 5, lower panel).

The change in the disintegration process can be conveniently characterized by $\tau_{\rm min}$, the minimum value that τ assumes as a function of the excitation energy. The region near $\tau_{\rm min}$ corresponds to the transition from channels with one big residual fragment to multifragmentation into several small fragments. In nuclear matter this transition is usually associated with the coexistence region of the liquid-gas phase transition. Both $\tau_{\rm min}$ and the corresponding effective temperature $T_{\rm min}$ vary as a function of the surface energy, as demonstrated in Fig. 6. As one can see, the three considered sources with different isospin content exhibit similar trends but the $\tau_{\rm min}$ for the neutron-rich sources is higher.

V. EXPERIMENTAL DATA ON THE τ PARAMETRIZATION OF THE CHARGE DISTRIBUTIONS

To extract information about the surface energy in multifragmentation we compare the calculations with experimental data. The ALADIN Collaboration has performed exclusive measurements of multifragmentation events for projectile-like sources with different isospins [1] and has made these data available. Measurements have been made with ^{238}U, ^{197}Au, and ^{129}Xe projectiles at a laboratory energy of 600 MeV per nucleon, interacting with different targets ranging from Be to U. The power-law parameters τ, obtained from fits to the

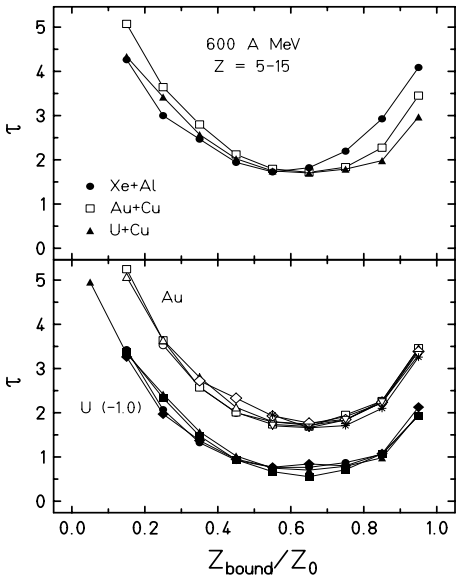

FIG. 7. Power-law parameters τ obtained from fitting the fragment charge distributions obtained in ALADIN experiments in the range $5 \leqslant Z \leqslant 15$ as a function of the reduced bound charge Z_{bound}/Z_0 for the fragmentation of ^{129}Xe, ^{197}Au, and ^{238}U projectiles of 600 MeV/nucleon. Top panel: three systems with different projectiles as indicated; bottom panel: results for collisions of ^{197}Au with Be, C, Al, Cu, In, and Au targets and of ^{238}U with Cu, In, Au, and U targets.

charge distributions in the range $5 \leqslant Z \leqslant 15$, are shown in Fig. 7 as a function of the bound charge Z_{bound} (the total charge accumulated in fragments with $Z \geqslant 2$) divided by the projectile charge Z_0. Small Z_{bound} values correspond to high excitation energies of the sources that disintegrate predominantly into very light clusters ("fall" of multifragmentation). Large values of Z_{bound} correspond to low excitation energies, at which the decay changes its character from evaporation-like or fission-like processes to multifragmentation ("rise" of multifragmentation).

The chosen target has no influence on the extracted τ parameter, as demonstrated in the bottom part of Fig. 7 for the case of the Au and U projectiles. This is consistent with the target invariance generally observed for the charge correlations of projectile fragmentation [1]. These invariance properties extend also to projectiles with different Z_0 if the data are scaled accordingly. For example, the IMF multiplicities divided by Z_0 (the reduced multiplicities) are practically identical if plotted as a function of the reduced bound charge Z_{bound}/Z_0. This has been shown in [1] for the case of U, Au, and Xe projectiles with the same data sets as used here. The same holds for the τ parameters, which, however, exhibit some variations at small and large Z_{bound} (Fig. 7, top). Differences at small Z_{bound} may occur for several reasons. The uncertainty of determining Z_{bound} for highly fragmented partitions, arising from the finite acceptance of the spectrometer for He and Li fragments [1], may be slightly system dependent, which, in principle, could be taken into account by using an experimental filter. Restricting Z_{bound} to small values will, furthermore, generate constraints for the accepted partitions that affect the resulting Z distributions [3]. The fitting within a fixed-Z interval while scaling Z_{bound} could thus possibly lead to systematic deviations in τ for different projectiles, which, however, are small, as evident from the data.

At large Z_{bound}, the observed differences are slightly larger and more systematic, and no experimental constraints of this type exist. The detection efficiency of the ALADIN spectrometer is, furthermore, very high for $Z \geqslant 5$, essentially 4π in the projectile frame, and the experimental trigger was adapted for the fragmentation channels [1]. In the following, we will, therefore, concentrate on the analysis of the observed differences in the behavior of τ for sources with different isospin at the "rise" of multifragmentation ($Z_{bound}/Z_0 \geqslant 0.5$). Because of the large acceptance of the detector, the theoretical predictions will be directly compared to the data without the use of an experimental filter.

VI. THEORETICAL CALCULATIONS WITH ENSEMBLES OF EQUILIBRATED SOURCES

In the most general consideration the fragmentation process can be subdivided into several stages as follows: (1) a dynamical stage leading to the formation of equilibrated nuclear systems, (2) disassembly of the system into individual primary fragments, and (3) de-excitation of hot primary fragments. Even though the first stage may be described by a dynamical model, such as the intranuclear cascade model, it is more practical to determine an ensemble of equilibrated sources, produced after the nonequilibrium stage, by direct comparison with experimental data [4]. In the following, we consider the ensembles of equilibrated sources extracted in Refs. [12,18] for the Au projectiles, which provide a very good description of the ALADIN data. We use the same version of the SMM code described fully in [5]. As was found in Ref. [12], the average masses of equilibrated sources A_s may be parametrized as $A_s/A_0 = 1 - a_1(E^*/A_s) - a_2(E^*/A_s)^2$, where E^* is the excitation energy of the sources in MeV, and A_0 is the projectile mass. Here $a_1 = 0.001$ MeV^{-1}, and $a_2 \approx 0.009$–0.015 MeV^{-2} slightly depends on the projectile energy. It should be noted that the adopted correlation of the mass number with the excitation energy is consistent with dynamical simulations [29,30], as well as with results of other statistical models [6,7,12]. Besides providing a very good description of fragment production at different Z_{bound}, the calculations with this kind of ensemble also correctly reproduce the behavior of the caloric curve [18].

Our present analysis is moderately sensitive to the relation between A_s and E^* because we extract τ in different Z_{bound}/Z_0 bins, which are correlated with the excitation energy (per nucleon) of the source. Possible variations of the relative weights of the sources in the ensembles have practically no effect on the τ observable, as was confirmed by performing calculations with different weights. The typical relative yields of sources used for the case of ^{197}Au projectiles are shown in Fig. 8 as a function of their mass and excitation energy. The parameter $a_2 = 0.012$ was used in this case. The same relation between masses and excitation energies is also taken for the other projectiles. It is assumed that the N/Z ratio of all sources in the ensemble is the same as in the projectiles.

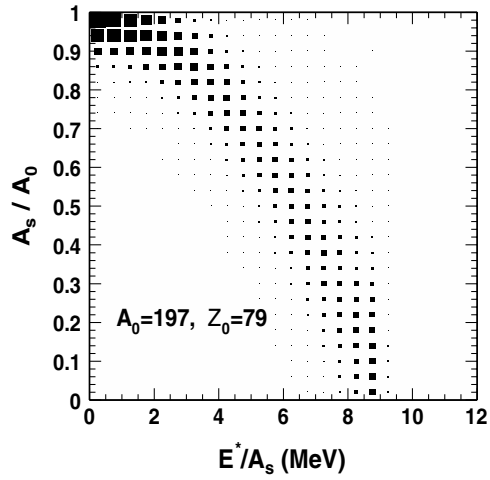

FIG. 8. Ensemble of hot thermal sources represented in a scatter plot of reduced mass number A_s/A_0 versus excitation energy E^*/A_s for the fragmentation of ^{197}Au projectiles, as used in the SMM calculations. The intensity of the individual sources is proportional to the area of the squares.

The dynamical calculations show that this is a quite reasonable assumption for sources with moderate excitation energies. A very small decrease of the N/Z ratio is predicted only for the sources with very high excitation energy [11,19]. This should not qualitatively influence the present analysis in the region of the multifragmentation rise.

The SMM calculations with these ensembles for different projectiles predict a scaling of the fragment multiplicities, as well as other observables, in agreement with the experimental data [1]. This is illustrated in Fig. 9, where we plot the reduced IMF multiplicities versus $Z_{\rm bound}/Z_0$. To demonstrate the sensitivity of this correlation to the ensemble parameters and to the surface energy, we compare calculations obtained with different parameter sets. For ^{197}Au we show results for the ensemble parameters $a_2 = 0.011$ (full squares) and $a_2 = 0.012$ (empty squares), obtained with the surface term $B_0 = 18$ MeV. For ^{238}U we compare the cases $B_0 = 17$ MeV (empty triangles) and $B_0 = 18$ MeV (full triangles) for ensembles

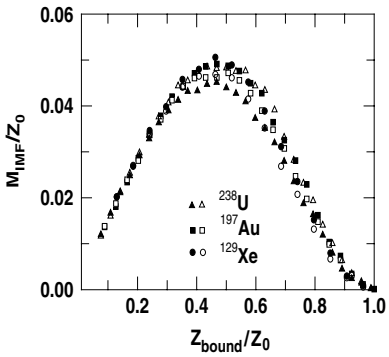

FIG. 9. Mean IMF multiplicities versus $Z_{\rm bound}/Z_0$, the bound charge divided by the projectile charge, predicted by the SMM ensemble calculations for three different projectiles. The meaning of the symbols is explained in the text.

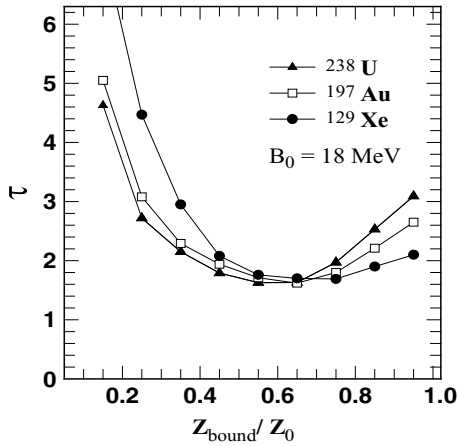

FIG. 10. SMM ensemble calculations of τ parameters for cold fragments versus $Z_{\rm bound}/Z_0$ for ^{238}U, ^{197}Au, and ^{129}Xe projectiles. The surface energy coefficient is $B_0 = 18$ MeV for all sources.

generated with $a_2 = 0.011$ and, for the ensembles representing the fragmentation of ^{129}Xe, generated with $a_2 = 0.012$, we show the results for $B_0 = 19$ MeV (full circles) and $B_0 = 20$ MeV (empty circles). In this way we cover the range of parameters representative for the following analysis of the data. One can clearly see a very good scaling behavior, similar to the experimental one demonstrated in Fig. 9 of Ref. [1]. A good description of the IMF multiplicities allows us to adjust the ensemble parameters and start the τ analysis. This analysis allows us to extract more detailed information on the multifragmentation process, since the τ fit in the range $Z = 5$–15 represents a new sensitive observable. It is important to mention that the maximum IMF production is reached at E^* around 5–6 MeV/nucleon, when the sizes of the sources are relatively large (Fig. 8).

The results of the SMM calculations for ensembles of the sources with $a_2 = 0.012$ produced with Xe, Au, and U projectiles are shown in Fig. 10. In the case of Au, the obtained τ parameters are close to the experimental values. This also remains valid in the region of the multifragmentation "fall" (i.e. at high excitation energies and small $Z_{\rm bound}$), even though the sources become small and have very large size variations (Fig. 8). However, in the region of the multifragmentation "rise" the theory gives larger τ for the neutron–rich U projectile than for the neutron-poor Xe projectile. This is opposite to the experimental observation. In the following we investigate possible modifications of the SMM that can explain this discrepancy.

First, we have tested whether one can improve the agreement with the experiment by simply using mass formulas with an explicit isospin dependence of the surface energy. We have implemented the Myers-Swiatecki mass formula [25] in the SMM, instead of the standard liquid-drop description of hot fragments. In this case the surface energy coefficient is written as $B_0 = 18.56[1 - 1.79(1 - 2Z/A)^2]$ MeV. The other parameters were also modified according to Ref. [25]. The results of the SMM calculations with the Myers-Swiatecki parametrization are shown in Fig. 11 for the ensembles with $a_2 = 0.012$ for all three projectiles. The resulting values of τ

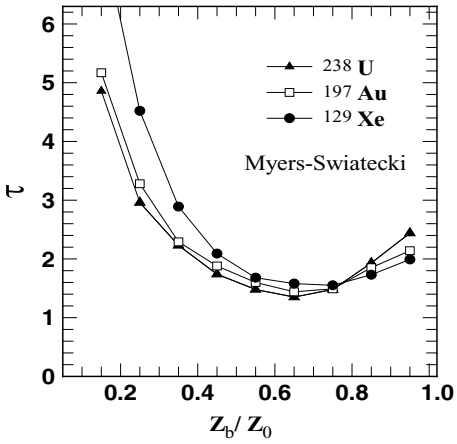

FIG. 11. SMM ensemble calculations of τ parameters for cold fragments versus Z_{bound}/Z_0 for ^{238}U, ^{197}Au, and ^{129}Xe projectiles. The Myers-Swiatecki mass formula was used for the hot primary fragments.

for different projectiles at large Z_{bound} have less of a spread than the results with constant $B_0 = 18$ MeV (Fig. 10) but they do not fit the experimental trend. Moreover, the general agreement with the experiment becomes even worse, since the minimum of τ is considerably shifted to larger values of Z_{bound}. Also, τ_{min} is less than 1.5, which is too low in comparison with the experimental value of about 1.7. Calculations with other ensembles did not improve the agreement with the experiment. This suggests that a more detailed investigation of the liquid-drop parameters of fragments in multifragmentation reactions is needed.

Returning to the standard SMM, we have performed calculations for the same projectile ensembles but with other surface coefficients B_0. We have selected four intervals, $Z_{\text{bound}}/Z_0 =$ 0.8–0.9, 0.7–0.8, 0.6–0.7, and 0.5–0.6, characterizing the "rise" of multifragmentation with excitation energy, for a detailed comparison with the experiment. As one can expect from Fig. 5, to fit the higher τ observed for neutron-poor Xe sources at low excitation energies, it is necessary to increase the surface coefficient B_0 for the corresponding hot fragments. As known from previous analyses (see, e.g., [27]), the secondary decay processes should not significantly influence τ in this region. For the secondary de-excitation calculations we have used the standard evaporation and Fermi breakup models implemented in the SMM [23]. The same de-excitation code was used in Refs. [12,18] for describing the ALADIN data.

The theoretical evolution of τ with B_0 in different Z_{bound} bins is shown in Fig. 12. To achieve agreement with the experimental data, B_0 should change with excitation energy when going from compound-like processes to full multifragmentation. In the bin of the largest $Z_{\text{bound}}/Z_0 = 0.85$, this requires $B_0 \approx 20.0$, 18.1, and 17.1 MeV for the Xe, Au, and U ensemble sources, respectively. At $Z_{\text{bound}}/Z_0 =$ $0.65A$ and $0.55A$, however, in the region of minimum τ and full multifragmentation, the values of the surface tension are around $B_0 \approx$ 18–19 MeV for all three sources without essential variation.

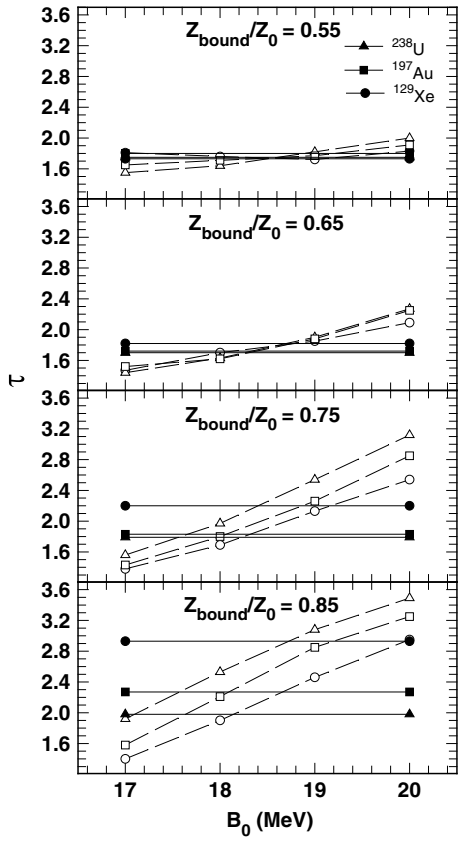

FIG. 12. Comparison of the τ parameters obtained from the SMM ensemble calculations as a function of B_0 (dashed lines and open symbols) with the experimental results (solid horizontal lines and full symbols) for U, Au, and Xe projectiles in different Z_{bound}/Z_0 bins.

We have also analyzed other ensembles and combinations of ensembles for different projectiles, which can reproduce the IMF scaling shown in Fig. 9 and in Ref. [1]. In addition, we require that these ensembles reproduce the experimental τ in the whole range of Z_{bound} by varying B_0. We have found that such ensembles should have parameters in between $a_2 =$ 0.011 and $a_2 = 0.013$. For control, we have also tested the extreme cases ($a_2 = 0.011$ for the ensembles of U sources and $a_2 = 0.013$ for the Xe sources). Even for these ensembles, we have obtained a similar evolution of the B_0 isospin dependence as a function of the excitation energy: Whereas B_0 depends strongly on N/Z at large Z_{bound}, it becomes nearly independent of isospin in the region of full multifragmentation.

Additional calculations were performed with another secondary decay code developed in Ref. [21]. This code starts with the modified surface tension for hot fragments in the freeze-out volume, and then changes the fragment masses during the evaporation process in such a way that the normal surface tension is restored for cold fragments. It was found that the final results may deviate from the standard calculations by not more than a few percent and that all trends regarding B_0 as a function of the neutron richness of fragments remain the same.

VII. DISCUSSION OF THE RESULTS

As was postulated earlier (Sec. IV), the surface term is a function of two parameters, B_0 and the critical temperature T_c. Therefore, a dependence of T_c on the neutron content could be an alternative explanation of the isospin dependence of the surface tension in different domains of excitation energy. This possibility was investigated by performing an analysis with a possible T_c evolution, as suggested in Refs. [27,28]. It was found that, to increase τ to the experimental value observed for Xe sources at large $Z_{\rm bound}$, T_c would have to be increased to $T_c \approx 24$ MeV. In the same $Z_{\rm bound}$ range, to reproduce the value for U sources, T_c would have to be decreased to $T_c \approx 14$ MeV. A T_c variation of this magnitude in a narrow N/Z range (from 1.39 to 1.59) is not supported by theoretical calculations [31], which predict a variation of T_c within 2%–3% only. In addition, large T_c differences for the projectile sources will result in a significant violation of the scaling behavior of fragmentation at high excitation energies, in contradiction to the experimental results.

We have mentioned that for small sources, at $Z_{\rm bound}/Z_0 < 0.5$, the experimental filter should be applied for a precise determination of $Z_{\rm bound}$ in simulated events. This would be important for our method since at high excitation energy, as one can see from Figs. 4 and 10, the τ extracted for the sources of different isospin nearly coincide, whereas the τ values after the ensemble calculations are different, when plotted versus the reduced bound charge. This is a consequence of dealing with the small sources and large fluctuations at the multifragmentation "fall." Also, in the region of small $Z_{\rm bound}$, after SMM calculations, many observables are less sensitive to differences in the ensembles of sources: As evident from Fig. 9, the slope of $M_{\rm IMF}/Z_0$ versus $Z_{\rm bound}/Z_0$ at small $Z_{\rm bound}$ is rather universal for all ensembles and values of B_0, and it coincides with the data [1]. Without independent constraints on the sources in this region, it is not very reliable to extract fragment properties by only using the τ parametrization of the charge yields. Probably, involving isotope distributions of produced fragments and measuring neutrons [32,33] will help to determine the ensembles. We do not touch this problem here but just note that extraction of B_0 as a function of the neutron richness at small $Z_{\rm bound}$ will depend essentially on the excitation energies of the sources. As one can see from Fig. 5 (bottom panel), if the average excitation energy is around 7–8 MeV/nucleon, the sensitivity of τ to the surface coefficient is lost at $B_0 \approx 18$–22 MeV.

Besides their different N/Z ratios, the three projectiles differ also in their mass. To first order, this is considered by performing the analysis as a function of scaled variables, but a residual mass effect may possibly exist. The calculations presented in Ref. [21] show, however, that for relatively large sources $A_s \sim 100$ a difference in the N/Z ratio has a larger effect on τ than a difference in the mass. Moreover, calculations for the fragmentation of nuclei with different N/Z and the same mass predict differences in τ of the same magnitude as obtained here for the considered Xe, Au, and U nuclei (Fig. 10). This justifies our conclusion that the deviation of the standard SMM calculations from the experimental data at low excitation energies is due to the isospin dependence of the surface coefficient. This conclusion can be tested with fragmentation data in experiments with isotopically different isobars.

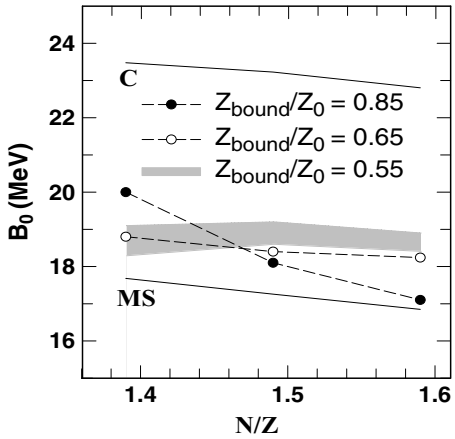

FIG. 13. The extracted B_0 for ensemble sources with different N/Z ratios at the onset ($Z_{\rm bound}/Z_0 = 0.85$ bin) and at the region of full multifragmentation ($Z_{\rm bound}/Z_0 = 0.65$ and 0.55 bins). The width of the shaded band represents limits given by our method for the lowest bin. The B_0 obtained from Cameron (C) and Myers-Swiatecki (MS) mass formulas for cold nuclei are shown by solid lines for illustration.

It is instructive to compare the surface coefficients extracted here with the ones used usually for cold isolated nuclei. In Fig. 13 we show the behavior of this coefficient versus the N/Z ratio as extracted from the Cameron [24] and Myers-Swiatecki [25] mass formulas by retaining terms proportional to $A^{2/3}$. The considered N/Z range corresponds to the neutron richness of the sources under investigation. Both mass formulas predict a decrease of B_0 with increasing N/Z, which is necessary to reach agreement with experimental mass tables. In multifragmentation, as was shown in Refs. [19,20,22], the neutron content of hot fragments is proportional to the neutron richness of the sources, since most neutrons are accumulated in the fragments. The values of B_0 extracted from the experiment exhibit the same decreasing trend with N/Z at low excitation energy and they remain within the B_0 range predicted by the mass formulas. Thus, at the rise of multifragmentation, when a heavy residue and few small fragments are formed, B_0 resembles the values used in phenomenological parameterizations for isolated nuclei. In contrast, at full multifragmentation, when the system breaks up into IMFs, the surface energy coefficient becomes nearly independent of the neutron richness. This is particularly evident for the bins $Z_{\rm bound}/Z_0 = 0.65$, where the decrease in B_0 with N/Z is very small, and $Z_{\rm bound}/Z_0 = 0.55$, at which the B_0 consistent with τ is represented by the shaded band (Fig. 13). Its width corresponds to the 2% statistical uncertainty in the numerical determination of τ, typical for both the SMM simulations and the experimental data.

These observations indicate that nuclear fragments are brought to a new physical environment. Their properties change in the hot medium, consisting of nucleons and other fragments at subnuclear freeze-out densities, around $0.1\rho_0$. Also, modifications of the symmetry energy have been

observed in these reactions [11]. Here, we do not suggest a comprehensive theoretical explanation of these effects, but rather we point at the new physical conditions reached in multifragmentation reactions in comparison with isolated nuclei. The origin of these effects could be a residual nuclear interaction between clusters, in particular, the exchange of neutrons between nuclear fragments. The role of Coulomb forces is also important. The Coulomb interaction between clusters leads to a modification of their average charges [23]. Other consequences of the Coulomb interaction, such as a shift of the proton distributions with respect to the neutron distributions in hot fragments [34], may additionally contribute to this effect.

Finally, we point to the uncertainty connected with the lack of knowledge of the N/Z ratio of the produced equilibrated sources after the initial dynamical stage. Present dynamical codes, such as the intranuclear cascade (INC) [19] and the relativistic Boltzmann Uehling Uhlenbeck (RBUU) [11,35], predict a very small, less than 5%, change in comparison with the neutron richness of the projectile nucleus. In this respect, the dynamical isospin fractionation [35] is less manifested in spectators produced in peripheral collisions at relativistic energies. This N/Z change is expected to be small for all projectiles; therefore, the difference in neutron content should be preserved for the ensembles of projectile sources. Similar conclusions can also be drawn on the basis of existing experimental data: As was established in recent ALADIN experiments, fragments coming from neutron-rich projectiles remain essentially neutron rich as compared with fragments from neutron-poor projectiles [32]. At the same time, the number of produced spectator neutrons is correlated directly with the neutron richness of the projectiles [33]. These results indicate that the initial difference in N/Z ratios for different projectiles is not washed out for the ensemble of sources during the nonequilibrium stage. Nevertheless, a direct experimental reconstruction of the neutron richness of the sources is desirable in the future [33].

VIII. CONCLUSIONS

In this paper we have demonstrated that the surface properties of hot fragments can be studied in multifragmentation reactions. Within the statistical multifragmentation model we have shown how modifications of the fragment surface energy influence the fragment production and thermodynamical characteristics of the system at the freeze-out volume. By comparing with the ALADIN data we have found that in the regime of the "rise" of multifragmentation the observed isospin dependence of the power-law parameter τ of fragment charge distributions cannot be described by the SMM if the standard surface-term coefficient is used. The data can be reproduced if a moderate dependence on the N/Z ratio of the produced fragments is introduced in the surface term. At low excitation energies this contribution resembles that obtained with advanced mass formulas for ground-state nuclei. At higher excitation energies, this N/Z dependence gradually disappears.

The observed modification of properties of hot nuclei in comparison with cold (or slightly excited) isolated nuclei are possibly caused by the hot environment in which the nuclei are imbedded, and where they can interact with nucleons and other fragments. The resulting in-medium modifications can go beyond the disappearance of shell effects and affect also the main liquid-drop parameters. Our conclusions are substantiated by a very good agreement with experimental data demonstrated by the SMM. In the future, fully microscopic calculations of the effects of the interacting medium would be very desirable; however, many problems still remain in constructing such a many-body theory.

More generally, we conclude that multifragmentation reactions offer a new possibility for investigating nuclei under conditions essentially different from those accessible in nuclear structure studies at low energies. Besides the obvious application of the results for better describing nuclear reactions at intermediate and high energies, this has far-reaching consequences for astrophysics. In many astrophysical situations, hot matter at subnuclear densities is clusterized into nuclei (e.g., in neutron star crusts and supernovae). The properties of these nuclei are crucial for both microscopic (weak interactions) and macroscopic (collapse dynamics and shock propagation) processes in stellar matter. New and important information in this direction may be expected from the analysis of future experimental data on multifragmentation.

ACKNOWLEDGMENTS

The authors would like to thank the ALADIN Collaboration for permission to use the charge-correlation data for the present analysis. A.B. thanks FIAS Frankfurt and GSI Darmstadt for support and hospitality, R.O. acknowledges the financial support by TUBITAK-DFG, and N.B. thanks Selcuk University-BAP(05401052) and GSI Darmstadt for financial support. This work was partly supported by Grant Nos. RFBR 05-02-04013 and NS-8756.2006.2 (Russia).

[1] A. Schüttauf *et al.*, Nucl. Phys. **A607**, 457 (1996).
[2] J. Pochodzalla and ALADIN Collaboration, Phys. Rev. Lett. **75**, 1040 (1995).
[3] P. Kreutz *et al.*, Nucl. Phys. **A556**, 672 (1993).
[4] A. S. Botvina and I. N. Mishustin, Phys. Lett. **B294**, 23 (1992).
[5] J. P. Bondorf, A. S. Botvina, A. S. Iljinov, I. N. Mishustin, and K. Sneppen, Phys. Rep. **257**, 133 (1995).
[6] B. A. Li, A. R. DeAngelis, and D. H. E. Gross, Phys. Lett. **B303**, 225 (1993).
[7] A. H. Raduta and A. R. Raduta, Phys. Rev. C **61**, 034611 (2000).
[8] H. A. Bethe, Rev. Mod. Phys. **62**, 801 (1990).
[9] A. S. Botvina and I. N. Mishustin, Phys. Lett. **B584**, 233 (2004).
[10] A. S. Botvina and I. N. Mishustin, Phys. Rev. C **72**, 048801 (2005).
[11] A. Le Fèvre *et al.*, Phys. Rev. Lett. **94**, 162701 (2005).
[12] A. S. Botvina *et al.*, Nucl. Phys. **A584**, 737 (1995).
[13] R. P. Scharenberg *et al.*, Phys. Rev. C **64**, 054602 (2001).
[14] L. Pienkowski *et al.*, Phys. Rev. C **65**, 064606 (2002).

[15] M. D'Agostino *et al*., Phys. Lett. **B371**, 175 (1996).
[16] N. Bellaize *et al*., Nucl. Phys. **A709**, 367 (2002).
[17] S. P. Avdeyev *et al*., Nucl. Phys. **A709**, 392 (2002).
[18] H. Xi *et al*., Z. Phys. A **359**, 397 (1997).
[19] A. S. Botvina, O. V. Lozhkin, and W. Trautmann, Phys. Rev. C **65**, 044610 (2002).
[20] D. V. Shetty *et al*., Phys. Rev. C **71**, 024602 (2005).
[21] N. Buyukcizmeci, R. Ogul, and A. S. Botvina, Eur. Phys. J. A **25**, 57 (2005).
[22] A. S. Botvina and I. N. Mishustin, Phys. Rev. C **63**, 061601(R) (2001).
[23] A. S. Botvina, A. S. Iljinov, I. N. Mishustin, J. P. Bondorf, R. Donangelo, and K. Sneppen, Nucl. Phys. **A475**, 663 (1987).
[24] A. G. W. Cameron, Can. J. Phys. **35**, 1021 (1957).
[25] W. D. Myers and W. J. Swiatecki, Nucl. Phys. **81**, 1 (1966).
[26] R. C. Nayak, Phys. Rev. C **60**, 064305 (1999).
[27] R. Ogul and A. S. Botvina, Phys. Rev. C **66**, 051601(R) (2002).
[28] V. A. Karnaukhov *et al*., Nucl. Phys. **A734**, 520 (2004).
[29] J. Konopka *et al*., Prog. Part. Nucl. Phys. **30**, 301 (1993).
[30] H. W. Barz *et al*., Nucl. Phys. **A561**, 466 (1993).
[31] D. G. Ravenhall *et al*., Nucl. Phys. **A407**, 571 (1983).
[32] C. Sfienti *et al*., Nucl. Phys. **A749**, 83c (2005).
[33] W. Trautmann *et al*., in *Proceedings of the International Workshop on Multifragmentation IWM2005, Catania, Italy, 2005,* edited by R. Bougault *et al*. (Italian Physical Society, Bologna, 2006), IPS Conf. Proc. Vol. **91**, p. 157.
[34] M. Jandel *et al*., J. Phys. G **31**, 29 (2005).
[35] T. Gaitanos *et al*., Nucl. Phys. **A732**, 24 (2004).